Durability of CaO–CaZrO3 Sorbents for High-Temperature CO2 Capture Prepared by a Wet Chemical Method

ARTICLE *in* ENERGY & FUELS · JANUARY 2014

Impact Factor: 2.79 · DOI: 10.1021/ef4020845

8 AUTHORS, INCLUDING:

Ming Zhao
Tsinghua University
18 PUBLICATIONS **245** CITATIONS
SEE PROFILE

Valerie Dupont
University of Leeds
60 PUBLICATIONS **996** CITATIONS
SEE PROFILE

S. J. Milne
University of Leeds
152 PUBLICATIONS **1,720** CITATIONS
SEE PROFILE

energy&fuels

Article

pubs.acs.org/EF

Durability of $CaO-CaZrO_3$ Sorbents for High-Temperature CO_2 Capture Prepared by a Wet Chemical Method

Ming Zhao,*[,†] Matthew Bilton,[†] Andy P. Brown,[†] Adrian M. Cunliffe,[‡] Emiliana Dvininov,[§] Valerie Dupont,[‡] Tim P. Comyn,[†] and Steven J. Milne[†]

[†]Institute for Materials Research, School of Process, Environmental and Materials Engineering (SPEME), and [‡]Energy Research Institute, School of Process, Environmental and Materials Engineering (SPEME), University of Leeds, Leeds LS2 9JT, United Kingdom

[§]MEL Chemicals, Swinton, Manchester M27 8LS, United Kingdom

Supporting Information

ABSTRACT: Powders of CaO sorbent modified with $CaZrO_3$ have been synthesized by a wet chemical route. For carbonation and calcination conditions relevant to sorbent-enhanced steam reforming applications, a powder of composition 10 wt % $CaZrO_3$/90 wt % CaO showed an initial rise in CO_2 uptake capacity in the first 10 carbonation−decarbonation cycles, increasing from 0.31 g of CO_2/g of sorbent in cycle 1 to 0.37 g of CO_2/g of sorbent in cycle 10 and stabilizing at this value for the remainder of the 30 cycles tested, with carbonation at 650 °C in 15% CO_2 and calcination at 800 °C in air. Under more severe conditions of calcination at 950 °C in 100% CO_2, following carbonation at 650 °C in 100% CO_2, the best overall performance was for a sorbent with 30 wt % $CaZrO_3$/70 wt % CaO (the highest Zr ratio studied), with an initial uptake of 0.36 g of CO_2/g of sorbent, decreasing to 0.31 g of CO_2/g of sorbent at the 30th cycle. Electron microscopy revealed that $CaZrO_3$ was present in the form of ≤0.5 μm cuboid and 20−80 nm particles dispersed within a porous matrix of $CaO/CaCO_3$; the nanoparticles are considered to be the principal reason for promoting multicycle durability.

INTRODUCTION

Powder sorbents for capturing CO_2 at high temperatures find applications in a number of areas. Calcium oxide is of interest for post-combustion capture (PCC) from fossil-fuel-fired power plants and other single-point industrial emitters.[1] Calcium-looping PCC based on the reversible reaction $CaO + CO_2 \leftrightarrows CaCO_3$ can be implemented using two parallel fluidized beds operated as a carbonator and a regenerative calciner, typically at ≥650 °C in ∼15% CO_2 and ≥950 °C in ∼100% CO_2, respectively.[2] Another area of application of CaO powder sorbents lies in steam reforming for the production of H_2, whereby removal of the CO_2 co-product shifts the reaction equilibrium in favor of greater H_2 yields and purity.[3] Conditions for carbonation are comparable to those of PCC, i.e., ∼600 °C in ∼15% CO_2; however, when oxygen looping is employed in sorption-enhanced steam reforming (SESR), overall enthalpy is reduced by the exchange of oxygen through a metal catalyst and the regeneration of the sorbent is carried out in air at temperatures of ≥800 °C.[4] Hence, sorbent regeneration conditions for SESR are considerably less severe than those for PCC, but nevertheless, unmodified CaO shows a serious loss of CO_2 capacity after repeated calcination cycles, leading to lower H_2 yields.[5,6] Thus, there is an economic need to develop high-reactivity CaO-based sorbents that maintain performance between 0.3 and 0.78 g of CO_2/g of sorbent over multiple CO_2 capture cycles for SESR applications.[7,8]

Improvements to CaO sorbents have been achieved by the addition of second-phase refractory "spacer" particles to inhibit densification of the CaO particle matrix.[6,9−20] It should be noted that refractory additives to CaO inhibit densification because of not merely physical separation of the sorbent particles but also differential thermal expansion effects and differential sintering rates of the two components, resulting in stresses that inhibit densification.[21] Table 1 shows examples of the multicycle performance of modified CaO sorbent powders under various looping conditions, which can be broadly categorized as "mild" calcination (≤800 °C, requiring very low CO_2 partial pressures for decarbonation) and "severe" calcination (>900 °C in the presence of high partial pressures of CO_2) conditions. Calcination conditions have a major effect on durability,[8] with increased calcination temperatures and dwell times giving increased densification, lower porosity, and lower CO_2 uptake within the time scale of each cycle (≥5 cycles); however, the preceding carbonation conditions also affect the degree of densification during calcination. Carbonate decomposition initially produces a porous structure: the more extensive the carbonation reaction, the greater the degree of porosity generated upon initial decarbonation, which can result in less densification at the completion of the calcination cycle. Near full carbonation (100% conversion ratio of CaO) is achievable within each cycle using relatively high temperatures, prolonged dwell times, and CO_2-rich atmospheres. Therefore, carbonation and decarbonation (calcination) conditions should both be considered when comparing durability performance data from different laboratories (Table 1). The multicycle reactivity of CaO is also affected by the steam content of the feed stream; steam treatments or other forms of hydration have been shown to improve performance because of structural

Received: October 19, 2013
Revised: January 17, 2014

   dx.doi.org/10.1021/ef4020845 | Energy Fuels XXXX, XXX, XXX−XXX

Table 1. Summary of Previous Reports on Spacer−CaO Sorbents

		carbonation			calcination				net CO_2 uptake ($gofCO_2/gofsorbent$)	
authors (reference)	sorbents (mass ratio)	atmosphere	T (°C)	t (min)	atmosphere	T (°C)	t (min)	number of cycles	initial	final
Li et al.[9]	75% CaO/25% $Ca_{12}Al_{14}O_{33}$	14% CO_2	690	30	100% N_2	850	10	13	0.40	0.45
		14% CO_2	690	30	20% CO_2	950	10	13	0.42	0.33
Martavaltzi and Lemonidou[10]	85% CaO/15% $Ca_{12}Al_{14}O_{33}$	15% CO_2	690	30	15% CO_2	850	5	45	0.45	0.36
	75% CaO/25% $Ca_{12}Al_{14}O_{33}$	15% CO_2	690	30	15% CO_2	850	5	45	0.35	0.3
Koirala et al.[11]	n_{Al}/n_{Ca} = 3:10	30% CO_2	700	10	30% CO_2	700	10	100	0.39	0.39
Broda and Muller[12]	n_{Al}/n_{Ca} = 1:9	55% CO_2	750	20	100% N_2	750	20	30	0.52	0.55
		100% CO_2	850	10	30% CO_2	950	10	100	0.36	0.25
Yu and Chen[13]	76% CaO/10% Al_2O_3/14% TiO_2	100% CO_2	750	60	100% N_2	750	30	15	0.40	0.36
Wu and Zhu[14]	90% CaO/10% TiO_2	20% CO_2	600	10	100% N_2	750	10	10	0.20	0.24
Li et al.[15]	58% CaO/42% MgO	100% CO_2	758	30	100% He	758	30	50	0.45	0.43
Derevschikov et al.[16]	20% CaO/80% Y_2O_3	25% CO_2	740	10	100% Ar	740	10	120	0.06	0.10
Zhao et al.[6]	65% CaO/35% SiO_2	67% CO_2	600	60	100% N_2	700	5	50	0.48	0.34
Lu et al.[17]	n_{Zr}/n_{Ca} = 3:10, by FSP[a]	30% CO_2	700	30	100% He	700	30	100	0.30	0.30
	n_{Zr}/n_{Ca} = 3:10, by FSP[a]	100% CO_2	850	10	30% CO_2	950	0	23	0.25	0.23
	n_{Zr}/n_{Ca} = 3:10, by FSP[a]	30% CO_2	750	10	100% He	750	10	50	0.31	0.32
	n_{Zr}/n_{Ca} = 3:10, by wet impregnation	30% CO_2	750	10	100% He	750	10	50	0.31	0.15
Koirala et al.[18]	n_{Zr}/n_{Ca} = 3:10 (41 wt % $CaZrO_3$)[b,c]	100% CO_2	700	30	100% He	700	30	100	0.34	0.33
	n_{Zr}/n_{Ca} = 5:10 (56 wt % $CaZrO_3$)[b,c]	100% CO_2	700	30	100% He	700	30	100	0.23	0.23
	n_{Zr}/n_{Ca} = 5:10 (56 wt % $CaZrO_3$)[b,c]	100% CO_2	850	10	30% CO_2	950	10	100	0.21	0.21
Radfarnia and Iliuta[19]	n_{Zr}/n_{Ca} = 3.03:10 (by a surfactant template ultrasound method)	100% CO_2	600	30	100% Ar	750	30	15	0.19	0.14
Broda and Muller[20]	n_{Zr}/n_{Ca} = 20:80 (36% ZrO_2/64% CaO)[d]	20% CO_2	650	20	100% CO_2	900	10	10	~0.33[e]	0.21
	n_{Zr}/n_{Ca} = 10:90 (20% ZrO_2/80% CaO)[d]	20% CO_2	650	20	100% CO_2	900	10	10	>0.49[f]	0.31
	n_{Zr}/n_{Ca} = 5:95 (10% ZrO_2/90% CaO)[d]	20% CO_2	650	20	100% CO_2	900	10	10	>0.57[f]	0.36

[a]FSP denotes "flame spray pyrolysis". [b]Prepared by the FSP method. [c]Phase percentage in mass was determined by quantification of powder XRD patterns. [d]Prepared by the sol−gel method: the precursor of CaO was $Ca(OH)_2$, and gelling time was 2 h. [e]The initial uptake was calculated by an average decay rate of 0.5% for a 10 cycle experiment. [f]The initial uptakes were not indicated in either the paper or the Supporting Information but are estimated to be >0.49 and >0.57 net CO_2 uptake (g of CO_2/g of sorbent) based on the average decay rate of >0.5% for a 10 cycle experiment.

changes associated with CaO ↔ $Ca(OH)_2$ interconversion.[22−24]

There has been considerable focus on the CaO/Al_2O_3 sorbent system because the *in situ* formation of $Ca_{12}Al_{14}O_{33}$ particles hinders densification and sintering of the CaO phase during calcination.[9−13] A number of other "spacer" particle additives are also reported, for example, CaO/$CaTiO_3$,[14] CaO/MgO,[15] CaO/Y_2O_3,[16] and CaO/SiO_2.[6] The performance of these materials is also summarized in Table 1.

Here, we report on the development of ZrO_2 as a potential stabilizer for CaO sorbents because the two components react at elevated temperatures to form a thermodynamically stable binary mixture of CaO and $CaZrO_3$.[17−20] Lu et al. employed a flame spray pyrolysis (FSP) technique to prepare zirconia-modified CaO sorbents.[17] They identified an optimum molar ratio n_{Zr}/n_{Ca} = 3:10 that retained a stable 64% molar conversion ratio (equal to a net CO_2 capture capacity of 0.30 g of CO_2/g of sorbent) after 23 cycles for calcination at 700 °C in He (carbonation at 700 °C in 30% CO_2 for 30 min). For a more severe calcination temperature of 950 °C, a greater change in uptake was observed, with the molar conversion ratio falling to 50% after 23 cycles.[17] Wet chemical synthesis of the same powder composition, n_{Zr}/n_{Ca} = 3:10, using co-precipitation from calcium nitrate and zirconyl nitrate solutions resulted in inferior performance compared to the FSP powder, such that the conversion ratio decreased from ~60 to 30% after 23 cycles. The difference was attributed to the lower surface area of the wet chemical powder.[17] The same group later reported that n_{Zr}/n_{Ca} = 5:10 powders prepared by the same method but containing 56 wt % $CaZrO_3$ gave optimum performance.[18] For very mild calcination conditions at 700 °C for 10 min in He (after carbonation in 100% CO_2), a conversion ratio of ~60% was retained after >100 cycles, equating to ~0.23 g of CO_2/g of sorbent. Increasing the calcination temperature to 950 °C (in 30% CO_2 after carbonation at 850 °C in 100% CO_2) showed a drop in performance relative to mild calcination, but nevertheless, a conversion ratio of ~55% was retained after 100 cycles.[18] Radfarnia and Iliuta produced Zr-modified CaO sorbents using a surfactant template ultrasound synthesis method.[19] The best powders, n_{Zr}/n_{Ca} = 3.03:10, exhibited a drop in the molar conversion ratio from ~32% in cycle 1 to ~24% in cycle 15. This corresponded to a CO_2 uptake of 0.19 g of CO_2/g of sorbent in cycle 1 and 0.14 g of CO_2/g of sorbent in cycle 15, for mild calcination at 750 °C in Ar, following carbonation at 600 °C in 100% CO_2.[19] Most recently, Broda and Muller have reported a sol−gel method using zirconium propoxide as the gelling agent.[20] Their best ZrO_2-stablized CaO sorbents were obtained using $Ca(OH)_2$ as a precursor for CaO and a gelling time of 2 h. Under relatively severe conditions (carbonation in 20% CO_2 at 650 °C for 20 min and calcination in 100% CO_2 at 900 °C for 10 min), the sorbents with the highest mass fraction of CaO (80 wt % CaO/20 wt % ZrO_2 and 90 wt % CaO/10 wt % ZrO_2) showed CO_2 uptakes at cycle 10 of 0.31 and 0.36 g of CO_2/g of sorbent, respectively. In contrast, the sorbents with a higher Zr mass fraction had a lower initial uptake but were more stable over multiple cycles,

dx.doi.org/10.1021/ef4020845 | Energy Fuels XXXX, XXX, XXX−XXX

for example, the uptake for 64 wt % CaO/36 wt % ZrO_2 decayed from an initial value of 0.33 to 0.21 g of CO_2/g of sorbent after 10 cycles.[20]

The present work concerns an alternative wet chemical powder synthesis method for $CaZrO_3$/CaO sorbent powders, tested over 30 carbonation−decarbonation cycles. We show that the overall performance is superior to other Zr-modified CaO sorbents produced by solution-precipitation routes: near-stable multicycle CO_2 capture performance, after an initial rise, is demonstrated for mild conditions relevant to SESR involving carbonation at 650 °C in 15% CO_2 and calcination in air at 800 °C. The sorbents are also evaluated under severe conditions relevant to PCC. Here, the capture capacity declines by <15% of the original value of 0.36 g of CO_2/g of sorbent by cycle 30. Scanning and transmission electron microscopy using selected area electron diffraction, atomic lattice imaging, and energy-dispersive X-ray spectroscopy with elemental mapping are used to investigate reasons for the favorable performance of the powders.

EXPERIMENTAL SECTION

A suspension of $Ca(OH)_2$ was prepared by adding 50 mmol of $Ca(OH)_2$ (Alfa Aesar) in 100 mL of ethanol dropwise to 100 mL of aqueous ammonium hydroxide solution (pH 11) under continuous stirring. The ZrO_2 precursor was prepared by dissolving $ZrO(NO_3)_2 \cdot xH_2O$ (Sigma-Aldrich) in amounts ranging from 2.52, 5.68, and 9.74 mmol in 50 mL of ethanol; this solution was then added dropwise to 50 mL of ammonium hydroxide solution (pH 11). The resulting hydrolyzed zirconyl nitrate sample was added dropwise to the $Ca(OH)_2$ suspension under vigorous stirring. The suspension was aged at room temperature for 3 h and then dried at 70 °C. The dried powders were calcined at 800 °C in air for 30 min. These samples are labeled "as-prepared" sorbent powders.

The as-prepared sorbents (3 mg) were subjected to multiple carbonation−decarbonation cycles (up to 30) in a thermogravimetric analyzer (TGA, Mettler Toledo TGA/DSC1 model) under severe and mild conditions to simulate SESR and PCC, respectively. For "mild" multicycle runs, the samples were purged in 15% CO_2 at 650 °C for carbonation and in air at 800 °C for calcination. For "severe" runs, 100% CO_2 was purged throughout each full cycle and carbonation−decarbonation cycling was realized by a temperature swing between 650 and 950 °C. For practical reasons, it was not possible to switch between 15% CO_2 during carbonation and 100% CO_2 during calcination using the equipment available; hence, it was necessary to alter the carbonation atmosphere for the severe condition. For both mild and severe conditions, heating and cooling rates were 20 °C/min, carbonation dwell times were 15 min, with no dwell period once the maximum calcination temperature was reached, and gas flow rates were 50 mL/min under dry conditions.

Powder X-ray diffraction (XRD) was employed to identify the phases present in the as-prepared powders and powders collected after TGA cycles, for 1, 5, 10, and 30 cycles. XRD data were collected using a Bruker D8 diffractometer (Cu Kα, λ = 1.5416 Å). The as-prepared powders (~1 g) were loaded in the 25 mm (diameter) well of a polymethylmethacrylate sample holder; for smaller quantities generated by the TGA experiments, the powders (~3 mg) were deposited on a silicon sample holder. It should be noted that there is some additional (Bragg) scattering from the silicon holder visible in the latter patterns. The resulting XRD patterns were analyzed using the X'Pert HighScore Plus software (version 3.0e). The positions, intensities, and shapes of the peaks were measured and matched to known powder diffraction files, using the International Centre for Diffraction Data (ICDD) PDF4 database. Rietveld refinements of the diffractograms were performed to quantify the mass fraction of phases present using the X'Pert HishScore Plus software. Details of the methods can be found elsewhere.[25,26]

The microstructure of carbonated and decarbonated sorbents was characterized by scanning electron microscopy (SEM) using LEO 1530 Gemini field emission gun (FEG)-SEM to scan the surface of the powder samples at 3 keV and a 3.7 mm working distance using an in-lens secondary electron detector. All samples for SEM were sputter-coated with a layer of platinum, ~5 nm thick. Transmission electron microscopy (TEM) was employed to gain insights into the detailed structure of the sorbent powders by selected area electron diffraction (SAED), atomic lattice imaging, energy-dispersive X-ray (EDX) spectroscopy, and elemental mapping. For this purpose, Philips CM200 FEG-TEM was operated at 197 keV and fitted with a Gatan imaging filter (GIF 200) and an Oxford Instruments 80 mm^2 X-Max silicon drift detector (SDD) EDX spectrometer running the AZTEC processing software. Samples were prepared by dispersing sorbents in ethanol and drop casting onto holey carbon TEM support films (Agar Scientific, Ltd.).

RESULTS AND DISCUSSION

The as-prepared sorbent powders contained a mixture of CaO (cubic) and $CaZrO_3$ (orthorhombic), as identified by powder XRD[27] (Figure 1). Rietveld refinement of the XRD data for as-prepared powders and powders after multiple TGA carbonation/decarbonation cycles gave residual (R_P) and weighted residual (R_{WP}) Rietveld parameters of <10% (see Figure S1 and Table S1 of the Supporting Information), indicating that the model provided a reliable indication of phase proportions (accurate to ±1 wt %).[22] The estimated weight fraction (%) of $CaZrO_3$ in the three as-prepared sorbents were as follows: sample 1, 10 $CaZrO_3$/90 CaO; sample 2, 18 $CaZrO_3$/82 CaO; and sample 3, 30 $CaZrO_3$/70 CaO. After 10 or 30 TGA cycles, each terminating with calcination, the equivalent CaO (CaO + $CaCO_3$) to $CaZrO_3$ mass ratios were the same as for the as-prepared powders, indicating that the initial calcination step had achieved complete reaction.

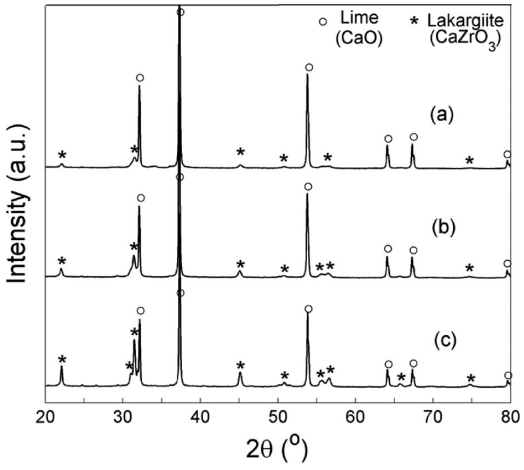

Figure 1. XRD patterns for the as-prepared sorbents (freshly calcined at 800 °C): (a) sample 1, 10 (wt %) $CaZrO_3$/90 (wt %) CaO; (b) sample 2, 18 $CaZrO_3$/82 CaO; and (c) sample 3, 30 $CaZrO_3$/70 CaO.

The net CO_2 uptakes, expressed as g of CO_2/g of total sorbent mixture, using the three as-prepared sorbent compositions under "mild" conditions are shown in Figure 2 (15% CO_2 at 650 °C for carbonation and in air at 800 °C); the specific CO_2 uptakes in cycles 1, 10, and 30 are listed in Table 2 accompanied with molar carbonation percentages of the CaO component, calculated according to eq 1.

dx.doi.org/10.1021/ef4020845 | Energy Fuels XXXX, XXX, XXX−XXX

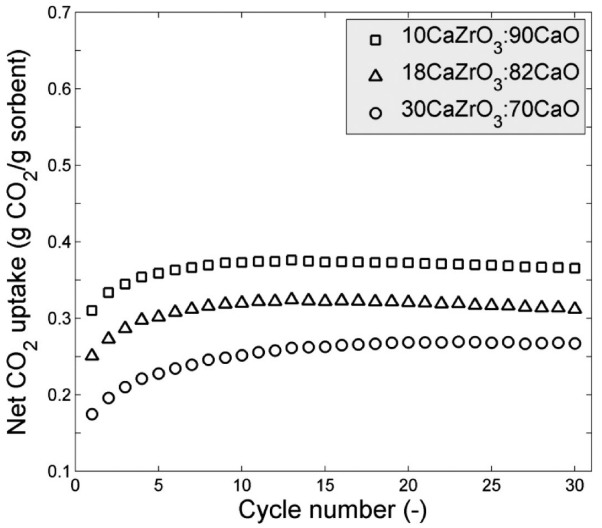

Figure 2. Cyclic CO_2 capture performance under the "mild" conditions (carbonation, 15% CO_2 at 650 °C for 15 min; calcination, air at 800 °C with no dwell time).

$$\text{carbonation (\%)} = 100 \times \left[\left(\text{net mass of } CO_2 \text{ uptake (g of } CO_2)/44\right) / \left(\text{CaO initial mass (g of CaO)}/56\right)\right] \quad (1)$$

Each of the sorbent blends showed an increase in uptake capacity in the first ~10 cycles, with little further variation over the full 30 cycles tested. For sample 1, the CO_2 uptake increased from 0.310 to 0.373 g of CO_2/g of sorbent between cycles 1 and 10, and for sample 2, the CO_2 uptake increased from 0.251 to 0.320 g of CO_2/g of sorbent between cycles 1 and 10. After cycle 10, a near-stable CO_2 uptake was demonstrated over the 30 cycles tested, retaining these capacities at cycle 30. For sample 3, a continuous increase was observed after cycle 10 and the CO_2 uptake reached 0.267 g of CO_2/g of sorbent. Sample 3 showed the lowest initial molar carbonation, 31.8%, of the three sorbents. However, after cycle 30, 48.5% of CaO in sample 3 was carbonated, in line with samples 1 and 2 (Table 2).

An initial increase in capacity has been observed for other CaO blends and is often referred to as "self-reactivation".[28] To understand this here, we chose to investigate the detailed microstructure of sample 3 because it exhibits the most significant increase in molar carbonation with cycles. The reasons behind this increase were revealed by SEM, which showed a densely packed microstructure with little porosity in the as-prepared powder, yet at cycle 10, the powder matrix was more porous, containing <100 nm pores within a matrix of <200 nm CaO particles (Figure 3). This development of a more porous matrix in the first 10 carbonation−calcination cycles accounts for the observed rise in CO_2 capacity; progressive changes to this microstructure in the earlier cycles would give rise to the gradual increase in CO_2 uptake that is observed.

A single TGA cycle for sample 3, the 30 $CaZrO_3$/70 CaO sorbent under the "mild" conditions (carbonation, 15% CO_2 at 650 °C for 15 min; calcination, air at 800 °C with no dwell time), for each of cycles 1, 5, 10, and 30 is shown in Figure 4. The most notable feature is the change in the TGA carbonation profile between cycles 1 and 5. No significant linear region is observed in cycle 1: the curvature to the profile over the full 15 min treatment and a t^n rate dependence over the total 18 wt % increase indicate that the carbonation kinetics are dominated by solid-state diffusion of CO_2 through a $CaCO_3$ layer.[29,30] By cycle 5, ~18 wt % of a total of 25 wt % mass gain in the carbonation step is associated with rapid linear kinetics, suggesting a surface reaction between CO_2 and exposed CaO particles.[29,30] Cycles 10 and 30 are very similar to cycle 5. The interpretation of these TGA profiles complements the microstructural observations by SEM (Figure 3): the carbonation in cycle 1 involves a densely packed powder, and therefore, only a very minor proportion of the total carbonation reaction occurs by the gas−solid reaction (linear kinetics) and the carbonation reaction is dominated by solid-state diffusion. For later cycles, the series of carbonation−decarbonation volume changing reactions has created porosity in the CaO powder (Figure 3). Most of this porosity will be created when the densified $CaCO_3$ particles decompose during calcination (Figure 5). Hence, a higher specific surface area becomes available for gas−solid chemical reactions, and a higher proportion of the carbonation reaction rate is controlled by the linear chemical kinetics of the surface reaction of CO_2 with CaO.

The multicycle results for severe calcination conditions, 950 °C in 100% CO_2, in which carbonation also occurred in 100% CO_2, are shown in Figure 6. As expected, carbonation in 100% CO_2 led to a greater molar conversion than in 15% CO_2. The cycle 1 CO_2 uptakes were 0.46, 0.43, and 0.36 g of CO_2/g of sorbent, for samples 1, 2, and 3, respectively. Sample 3 with its increased $CaZrO_3$ content of 30 wt % was studied because of its better durability under severe conditions than for samples 1 and 2; i.e., it shows the lowest decline in capture capacity (Figure 6) and the greatest percentage of carbonation (Table 3). A decline in capture capacity over prolonged cycling occurred for these severe calcination conditions; this is in contrast to the very stable performance in prolonged multicycle operation for mild calcination at 800 °C. For example, the uptake decayed from 0.36 g of CO_2/g of sorbent at cycle 1 to 0.31 g of CO_2/g of sorbent by cycle 30 for sample 3, representing a decline of <14% of the initial value (Table 3). Examination of SEM micrographs indicated an increased degree of interparticle

Table 2. Net CO_2 Uptakes and Carbonation Percentages for Cycles 1, 10, and 30 under "Mild" Conditions (Carbonation, 15% CO_2 at 650 °C for 15 min; Calcination, Air at 800 °C with No Dwell Time)

	carbonation			calcination			net CO_2 uptake (g of CO_2/g of sorbent)			carbonation (%)		
	gas	T (°C)	t (min)	gas	T (°C)	t (min)	1st	10th	30th	1st	10th	30th
10 $CaZrO_3$/90 CaO	15% CO_2	650	15	air	800	0	0.310	0.373	0.365	43.8	52.7	51.6
18 $CaZrO_3$/82 CaO							0.251	0.320	0.312	39.0	49.7	48.4
30 $CaZrO_3$/70 CaO							0.175	0.251	0.267	31.8	45.6	48.5

dx.doi.org/10.1021/ef4020845 | Energy Fuels XXXX, XXX, XXX−XXX

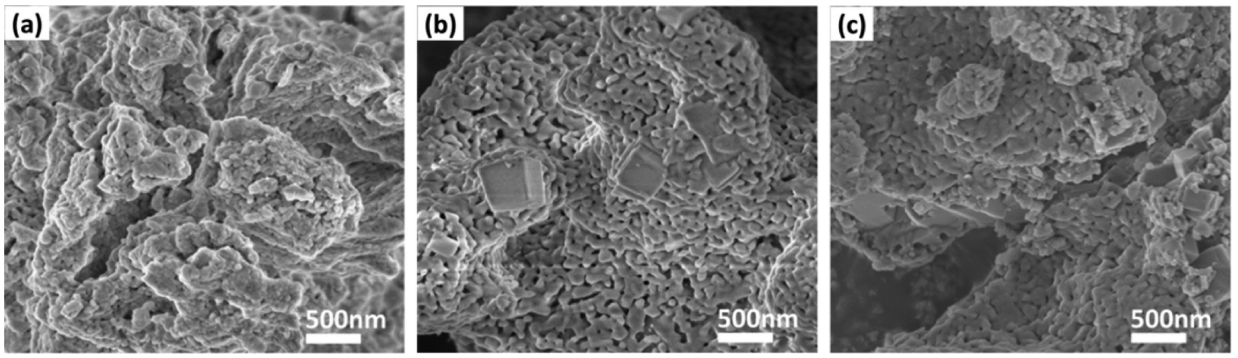

Figure 3. SEM images of porosity development within sample 3, the 30 $CaZrO_3$/70 CaO sorbent after the "mild" TGA cycles, ending on calcination (carbonation, 15% CO_2 at 650 °C for 15 min; calcination, air at 800 °C with no dwell time): (a) fresh form, (b) after 10 cycles, and (c) after 30 cycles. The cuboid particles evident in panels b and c are identified as $CaZrO_3$ microparticles by TEM (Figure 8).

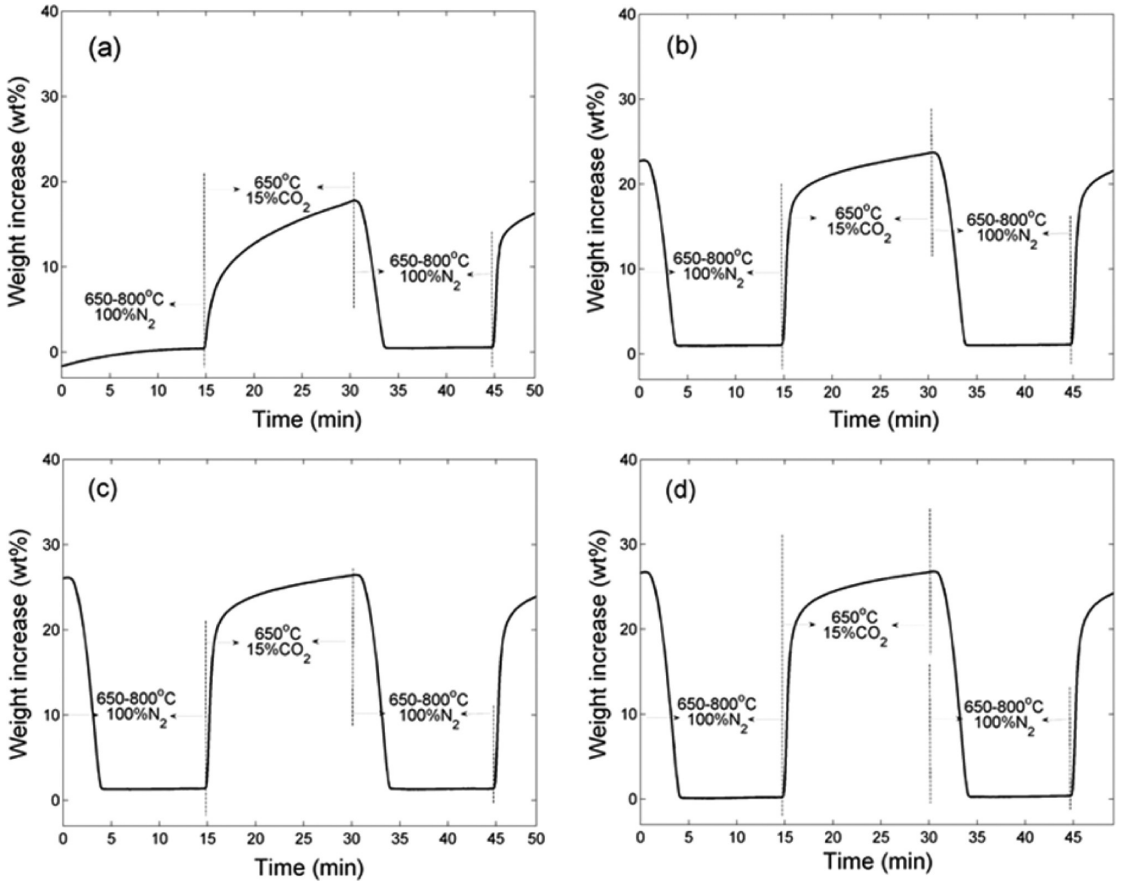

Figure 4. TGA weight profiles with time for sample 3, the 30 $CaZrO_3$/70 CaO sorbent under the "mild" conditions (carbonation, 15% CO_2 at 650 °C for 15 min; calcination, air at 800 °C with no dwell time), for (a) cycle 1, (b) cycle 5, (c) cycle 10, and (d) cycle 30. Note that the initial baseline drift of the TGA (first cycle in panel a) stabilizes after one complete cycle.

necking with an increasing number of calcination cycles and a slight increase in particle size (relative to the mild conditions) (Figure 7). The resulting reduction in solid−gas interfacial area, cycle-on-cycle, gives rise to the decrease in uptake capacity.

Examples of TEM analysis of as-prepared powders and powders after multiple TGA mild cycles are shown in Figure 8. Elemental Zr mapping of a group of particles in an as-prepared powder (Figure 8a) highlights a Zr-rich region ∼150 nm in size that corresponds to one of the $CaZrO_3$ cuboid particles first identified by SEM (Figure 3). Much smaller Zr-containing regions were also identified, dispersed throughout the matrix: SAED (not shown) and lattice imaging revealed these Zr signals were due to nanoscale particles of $CaZrO_3$, 20−80 nm in size, distributed within the ≤200 nm CaO particle matrix (Figure 8b). Particles after 10 and 30 cycles (ending with calcination) are shown in panels c and d of Figure 8, respectively. The EDX elemental mapping implies that some intraparticle segregation of $CaZrO_3$ nanoparticles may have occurred upon repeat cycling, but this did not affect durability in the mild cycles (Figure 2). It is assumed that the near-stable CO_2 capture durability from the $CaZrO_3$/CaO powders is principally due to these $CaZrO_3$ nanoparticles acting as spacers to suppress densification and loss of micro- or mesoporosity during repeated calcinations. While it is possible that a very

dx.doi.org/10.1021/ef4020845 | Energy Fuels XXXX, XXX, XXX−XXX

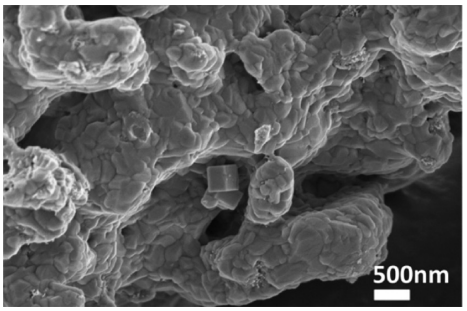

Figure 5. SEM image of the densified microstructure of sample 3, the 30 $CaZrO_3$/70 CaO sorbent after 10 "mild" TGA cycles (carbonation, 15% CO_2 at 650 °C for 15 min; calcination, air at 800 °C with no dwell time), when ending on carbonation.

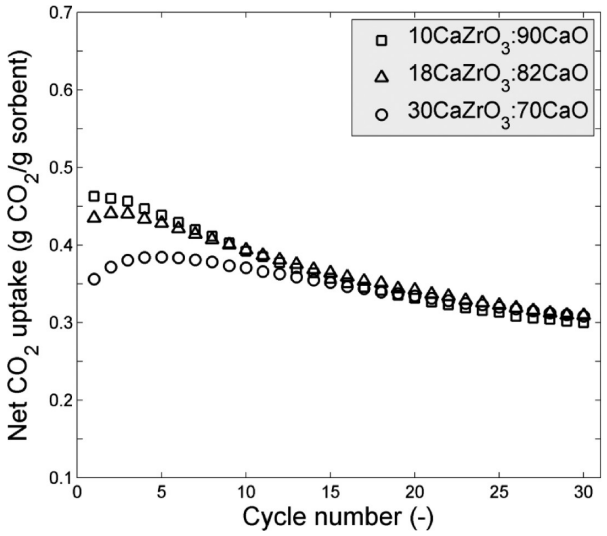

Figure 6. Cyclic CO_2 capture performance under the "severe" conditions (carbonation, 100% CO_2 at 650 °C for 15 min; calcination, 100% CO_2 at 950 °C with no dwell time).

limited range of solid solution (<1%) forms between CaO and ZrO_2,[31] there was no evidence of this from XRD lattice spacing measurements.

Powders from FSP were reported to have optimal durability at n_{Zr}/n_{Ca} = 3:10[17] and later revised to the more dilute blend n_{Zr}/n_{Ca} = 5:10,[18] containing 56% $CaZrO_3$. This is almost double the amount of $CaZrO_3$ in sample 3 of the present work, yet the initial molar conversion ratios are similar, probably because of the smaller CaO particle size from FSP and the higher temperatures and CO_2 partial pressures used for the carbonation step in the FSP trials. Both powder types display comparable durability under mild conditions, but the FSP shows slightly better stability at higher temperatures probably in part because of the higher $CaZrO_3$ content. The overall performance of the present powders is superior in terms of initial uptake capacity and multicycle durability when compared to several other Zr-modified CaO powders produced by wet chemical routes.[17,19] The new powders presented here show negligible decay in CO_2 capacity within the 30 cycles tested under decarbonation at 800 °C: a mere 2% decrease was observed in net CO_2 uptake from cycle 10 to cycle 30, and near-flat molar conversion ratios of >50% were recorded for sample 1, the 10 $CaZrO_3$/90 CaO sorbent (Table 2). A co-precipitation method, from Zr and Ca salt solutions, produced powders that showed a drop in conversion ratio from >60 to ~40% after 10 cycles and falling further to ~35% after 30 mild calcination cycles at 750 °C.[17] Another wet chemical method based on a surfactant template ultrasound chemical route showed an initial uptake of only 0.19 g of CO_2/g of sorbent in cycle 1 decaying to 0.14 g of CO_2/g of sorbent in cycle 15 for calcination temperatures 750 °C[19] compared to an uptake stabilizing at 0.37 g of CO_2/g of sorbent in this work. A sorbent produced by a sol–gel synthesis route with n_{Zr}/n_{Ca} = 20:80, containing 36 wt % ZrO_2 (equivalent to 52 wt % $CaZrO_3$/48 wt % CaO assuming full conversion), exhibited an initial capacity of 0.33 g of CO_2/g of sorbent decreasing to 0.21 g of CO_2/g of sorbent at cycle 10. This represents a relative decline of 36% in 10 cycles (carbonation in 20% CO_2 at 650 °C for 20 min and calcination in 100% CO_2 at 900 °C for 10 min).[20] The uptake of the present 30 wt % $CaZrO_3$/70 wt % CaO sorbent (carbonation in 100% CO_2 at 650 °C and calcination in 100% CO_2 at 950 °C) increased slightly from 0.36 (initial) to 0.39 g of CO_2/g of sorbent (cycle 4) and then steadily decayed to 0.37 g of CO_2/g of sorbent at cycle 10, reaching 0.31 g of CO_2/g of sorbent at cycle 30, representing a decrease of ~14% over 30 cycles. It should be noted that the wet chemical method described in this work is relatively simple in comparison to other methods, such as FSP, ultrasound-assisted surfactant template synthesis, and sol–gel synthesis, which will have a favorable impact on processing costs.

In terms of comparisons between the present $CaZrO_3$/CaO powders and other CaO-based sorbent compositions, an optimum 25 wt % $Ca_{12}Al_{14}O_{33}$/75 wt % CaO blend maintained an uptake of 0.45 g of CO_2/g of sorbent for up to 13 "mild" cycles for calcination at 850 °C in N_2 for 10 min (Table 1).[9] Martavaltzi and Lemonidou[10] reported similar performance for this type of sorbent. When calcination temperatures are raised to 950 °C, which are more realistic for PCC applications, capacity decayed from 0.4 to 0.33 g of CO_2/g of sorbent after 13 cycles. This compares to a change from 0.36 to 0.31 g of CO_2/g of sorbent after 30 cycles for 30 $CaZrO_3$/70 CaO (sample 3); this capacity at 30 cycles is much higher than the data extrapolated to 30 cycles by Li et al.[9] Koirala et al.[11] synthesized a $Ca_{12}Al_{14}O_{33}$/CaO sorbent (n_{Al}/n_{Ca} = 3:10) by a single-nozzle FSP method and reported near-stable CO_2 uptake to the 100th cycle of ~0.40 g of CO_2/g of sorbent for mild

Table 3. Net CO_2 Uptakes and Carbonation Percentages for Cycles 1, 10, and 30 under the "Severe" Conditions (Carbonation, 100% CO_2 at 650 °C for 15 min; Calcination, 100% CO_2 at 950 °C with No Dwell Time)

	carbonation			calcination			net CO_2 uptake (g of CO_2/g of sorbent)			carbonation (%)		
	gas	T (°C)	t (min)	gas	T (°C)	t (min)	1st	10th	30th	1st	10th	30th
10 $CaZrO_3$/90 CaO	100% CO_2	650	15	100% CO_2	950	0	0.46	0.39	0.30	65.4	55.4	42.4
18 $CaZrO_3$/82 CaO							0.43	0.39	0.31	69.1	62.6	49.2
30 $CaZrO_3$/70 CaO							0.36	0.37	0.31	64.7	67.4	56.1

dx.doi.org/10.1021/ef4020845 | Energy Fuels XXXX, XXX, XXX–XXX

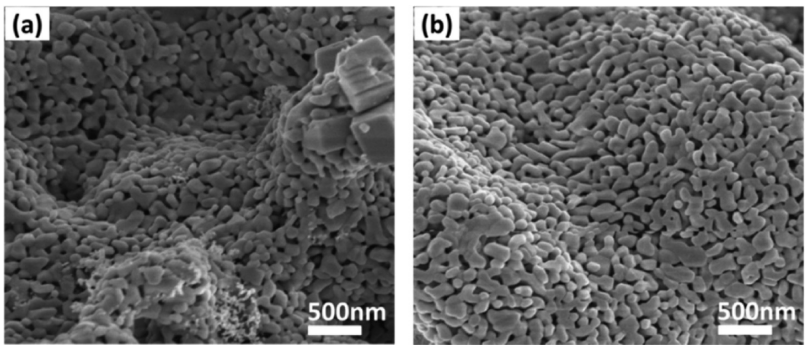

Figure 7. SEM images of the particle growth and necking for sample 3, the 30 $CaZrO_3$/70 CaO sorbent after the "severe" TGA cycles, ending on calcination (carbonation, 15% CO_2 at 650 °C for 15 min; calcination, air at 800 °C with no dwell time): (a) after 10 cycles and (b) after 30 cycles.

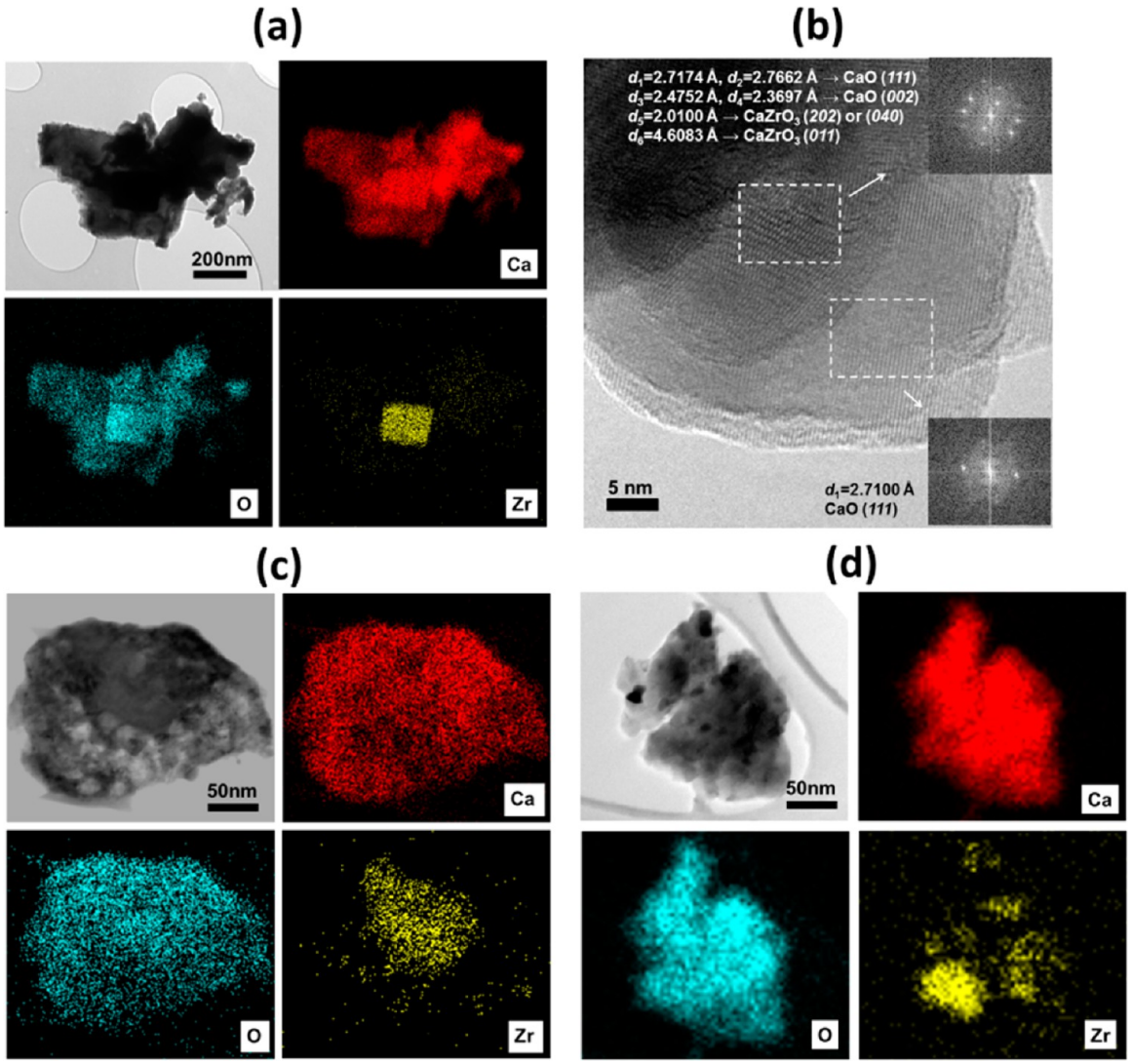

Figure 8. TEM analysis of sample 3, the 30 $CaZrO_3$/70 CaO sorbent: (a) TEM bright-field image and associated elemental X-ray maps for the freshly calcined sorbent, (b) atomic lattice image and inset Fourier transforms indexed to CaO or $CaZrO_3$ phases for the freshly calcined sorbent, (c) TEM bright-field image and associated elemental X-ray maps for the spent sorbent from cycle 10 under the "mild" conditions, ending on calcination, and (d) TEM bright-field image and associated elemental X-ray maps for the spent sorbent from cycle 30 under the "mild" conditions, ending with calcination.

calcination at 700 °C for 10 min, but this decreased to 0.25 g of CO_2/g of sorbent for calcination at 950 °C for 10 min in 30% CO_2. Broda and Muller have prepared a $Ca_{12}Al_{14}O_{33}$/CaO sorbent using a sophisticated organic template synthesis method, in which particle sizes were ∼170 nm.[12] The resorcinol/formaldehyde and aqueous Ca−Al precursors underwent a 3 day gelation, followed by calcination in an inert atmosphere, which formed nanosized carbonaceous

dx.doi.org/10.1021/ef4020845 | Energy Fuels XXXX, XXX, XXX−XXX

spheres coated with Ca−Al species. Hollow spherical calcium oxide/calcium aluminate particles were obtained after removing the carbon templates. The improved microstructure enabled a near-stable performance for up to 30 cycles for calcination at 750 °C in N_2 with a capacity of ∼0.55 g of CO_2/g of sorbent. However, the complicated production of the sorbent can hardly be realized at larger scales.

Yu and Chen[13] modified a $Ca_{12}Al_{14}O_{33}$-stabilized CaO sorbent powder (n_{Al}/n_{Ca} = 3:10) using an additional TiO_2 binder. A drop from 0.40 to 0.36 g of CO_2/g of sorbent (n_{Al}/n_{Ca} = 3:10) was reported for a long carbonation time, 60 min, and calcination at 750 °C for 30 min in N_2. Such long reaction times are not feasible for industrial operations.

Wu and Zhu[14] used 17 wt % $CaTiO_3$ as a spacer to maintain a stable CO_2 uptake at 0.23 g of CO_2/g of sorbent over 10 mild reaction cycles for calcination at 750 °C for 10 min in N_2. Li et al.[15] used 42 wt % MgO in CaO and attained stable uptake of ∼0.43 g of CO_2/g of sorbent over 50 cycles for calcination temperatures of 758 °C (and carbonation times of 30 min). Derevschikov et al.[16] added 80 wt % Y_2O_3 to CaO powders to obtain a very stable sorbent but with a net CO_2 uptake capacity of only ∼0.1 g of CO_2/g of sorbent (calcination at 740 °C for 10 min in argon). Zhao et al.[6] used 33 mol % SiO_2 as a stabilizer to produce a performance that dropped from 0.48 to 0.34 g of CO_2/g of sorbent over 50 mild reaction cycles at 700 °C for ≤60 min.

Overall, the present powders compare favorably in terms of multicycle sorbent performance to previously reported CaO-based materials. The key to further improving the high-temperature durability of $CaZrO_3$/CaO lies in refining solution synthesis conditions to reduce the proportion of cuboid $CaZrO_3$ microparticles and maximize the proportion of $CaZrO_3$ nanoparticles within the CaO matrix.

CONCLUSION

Powder sorbents of CaO modified with $CaZrO_3$ were prepared in three different component ratios, as identified by Rietveld refinement of XRD data: 10, 18, and 30 wt % $CaZrO_3$. The CO_2 capture performance was evaluated over 30 carbonation/decarbonation cycles for two sets of conditions. The overall performance of the powders compares favorably to other Zr-modified CaO powders produced by different wet chemical routes. Near-stable multicycle CO_2 uptake was demonstrated for calcination at 800 °C in air after prolonged thermal cycling (30 cycles tested). For example, a CO_2 uptake capacity of 0.373 g of CO_2/g of sorbent (for cycle 10) decreasing very slightly to 0.365 g of CO_2/g of sorbent (for cycle 30) was demonstrated for a 10 (wt %) $CaZrO_3$/90 (wt %) CaO powder blend. These powders may prove to be useful in SESR applications. Under severe calcination conditions, 950 °C in 100% CO_2 (calcination at 650 °C in 100% CO_2 for 15 min), the most durable composition, 30% $CaZrO_3$/70% CaO, demonstrated an uptake of 0.36 g of CO_2/g of sorbent in cycle 1, decreasing to 0.31 by cycle 30.

ASSOCIATED CONTENT

Supporting Information

Quality of Rietveld refinement for the as-prepared and cycled sorbent powders (Figure S1 and Table S1). This material is available free of charge via the Internet at http://pubs.acs.org.

AUTHOR INFORMATION

Corresponding Author

*Telephone: +44-113-343-8592. E-mail: simon.ming.zhao@gmail.com.

Notes

The authors declare no competing financial interest.

ACKNOWLEDGMENTS

The authors acknowledge the financial support of the Engineering and Physical Sciences Research Council (EPSRC) for Grant EP/J014702/1.

REFERENCES

(1) Anthony, E. J.; Bulewicz, E. M.; Jia, L. *Prog. Energy Combust. Sci.* **2007**, *33* (2), 171−210.
(2) Abanades, J. C.; Anthony, E. J.; Wang, J.; Oakey, J. E. *Environ. Sci. Technol.* **2005**, *39* (8), 2861−2866.
(3) Dou, B.; Dupont, V.; Rickett, G.; Blakeman, N.; Williams, P. T.; Chen, H.; Ding, Y.; Ghadiri, M. *Bioresour. Technol.* **2009**, *100* (14), 3540−3547.
(4) Pimenidou, P.; Rickett, G.; Dupont, V.; Twigg, M. V. *Bioresour. Technol.* **2010**, *101* (23), 9279−9286.
(5) Ramkumar, S.; Phalak, N.; Fan, L.-S. *Ind. Eng. Chem. Res.* **2011**, *51* (3), 1186−1192.
(6) Zhao, M.; Yang, X.; Church, T. L.; Harris, A. T. *Environ. Sci. Technol.* **2012**, *46* (5), 2976−2983.
(7) MacKenzie, A.; Granatstein, D. L.; Anthony, E. J.; Abanades, J. C. *Energy Fuels* **2007**, *21* (2), 920−926.
(8) Manovic, V.; Charland, J. P.; Blamey, J.; Fennell, P. S.; Lu, D. Y.; Anthony, E. J. *Fuel* **2009**, *88* (10), 1893−1900.
(9) Li, Z.-s.; Cai, N.-s.; Huang, Y.-y.; Han, H.-j. *Energy Fuels* **2005**, *19* (4), 1447−1452.
(10) Martavaltzi, C. S.; Lemonidou, A. A. *Ind. Eng. Chem. Res.* **2008**, *47* (23), 9537−9543.
(11) Koirala, R.; Reddy, G. K.; Smirniotis, P. G. *Energy Fuels* **2012**, *26* (5), 3103−3109.
(12) Broda, M.; Müller, C. R. *Adv. Mater.* **2012**, *24* (22), 3059−3064.
(13) Yu, C.-T.; Chen, W.-C. *Powder Technol.* **2013**, *239*, 492−498.
(14) Wu, S. F.; Zhu, Y. Q. *Ind. Eng. Chem. Res.* **2010**, *49* (6), 2701−2706.
(15) Li, L.; King, D. L.; Nie, Z.; Howard, C. *Ind. Eng. Chem. Res.* **2009**, *48* (23), 10604−10613.
(16) Derevschikov, V. S.; Lysikov, A. I.; Okunev, A. G. *Ind. Eng. Chem. Res.* **2011**, *50* (22), 12741−12749.
(17) Lu, H.; Khan, A.; Pratsinis, S. E.; Smirniotis, P. G. *Energy Fuels* **2008**, *23* (2), 1093−1100.
(18) Koirala, R.; Gunugunuri, K. R.; Pratsinis, S. E.; Smirniotis, P. G. *J. Phys. Chem. C* **2011**, *115* (50), 24804−24812.
(19) Radfarnia, H. R.; Iliuta, M. C. *Ind. Eng. Chem. Res.* **2012**, *51* (31), 10390−10398.
(20) Broda, M.; Müller, C. R. *Fuel* **2014**, DOI: 10.1016/j.fuel.2013.08.004.
(21) Vasconcelos, C. New challenges in the sintering of HA/ZrO_2 composites. In *Sintering of Ceramics—New Emerging Techniques*; Lakshmanan, A., Ed.; InTech: Rijeka, Croatia, 2012.
(22) Molinder, R.; Comyn, T. P.; Hondow, N.; Parker, J. E.; Dupont, V. *Energy Environ. Sci.* **2012**, *5* (10), 8958−8969.
(23) Donat, F.; Florin, N. H.; Anthony, E. J.; Fennell, P. S. *Environ. Sci. Technol.* **2011**, *46* (2), 1262−1269.
(24) Blamey, J.; Lu, D. Y.; Fennell, P. S.; Anthony, E. J. *Ind. Eng. Chem. Res.* **2011**, *50* (17), 10329−10334.
(25) Meethong, N.; Huang, H. Y. S.; Speakman, S. A.; Carter, W. C.; Chiang, Y. M. *Adv. Funct. Mater.* **2007**, *17* (7), 1115−1123.
(26) Wang, Z.; Comyn, T. P.; Ghadiri, M.; Kale, G. M. *J. Mater. Chem.* **2011**, *21*, 16494−1649.
(27) CaO, ICDD-PDF-04-011-8430 (lime, syn); $CaZrO_3$, ICDD-PDF-04-010-6396 (lakargiite, syn).

(28) Manovic, V.; Anthony, E. J. *Int. J. Environ. Res. Public Health* **2010**, *7* (8), 3129−3140.
(29) Florin, N. H.; Harris, A. T. *Energy Fuels* **2008**, *22* (4), 2734−2742.
(30) Yang, Z.; Zhao, M.; Florin, N. H.; Harris, A. T. *Ind. Eng. Chem. Res.* **2009**, *48* (24), 10765−10770.
(31) Du, Y.; Jin, Z.; Huang, P. *J. Am. Ceram. Soc.* **1992**, *75* (11), 3040−3048.